Comparative study of charge carrier mobility effect on the performance of conventional P_3HT:PCBM based bulk hetero-junction organic solar cells

ALIASGHAR AYOBI*
Department of Physics, Bojnourd Branch, Islamic Azad University, Bojnourd, Iran

In this work the effects of charge carriers mobility on the performance of P3HT:PCBM based bulk hetero-junction (BHJ) organic solar cells (OSCs) has been investigated. For this purpose, the simulation tool ATLAS-SILVACO package based on drift-diffusion approximation has been used. The simulation results indicate that with increasing charge carriers mobility, short circuit current density (Jsc) of BHJ OSCs has been increased. Also with considering a constant value for hole mobility and increasing the electron mobility, open circuit voltage (V_{oc}) of BHJ OSCs has been decreased. While with considering a constant value for electron mobility and increasing the hole mobility, V_{oc} has been increased. In the case of power conversion efficiency (PCE) of BHJ OSCs, the simulation results indicate that with considering an average value for mobility of one charge carrier and increasing the mobility of other charge carrier, the PCE of devices has been increased gradually towards the optimum point. But after this point, the PCE has been decreased. Also, the fill factor (FF) of BHJ OSCs has been increased with increasing the mobility of charge carriers due to decreasing of direct recombination rate.

(Received September 17, 2024; accepted August 4, 2025)

Keywords: Mobility, Bulk hetero-junction, Organic solar cell, Open circuit voltage, Short circuit current, Power conversion efficiency, Fill factor

1. Introduction

Much attention has been attracted to cheaper electric power production with using organic and inorganic solar cells in recent years [1,2]. However organic solar cells (OSCs) have many benefits compared to inorganic solar cells (IOSCs) due to their low cost production, increased production speed, light weight, flexibility, and high absorption coefficient [3-5]. The fundamental problem of OSCs is that often are unstable under the influence of environmental cyclic changes and steady operation cannot be provided during performance lifetime [6]. Also, in OSCs there are significant degradations in layers and interfaces. Therefore, in order to obtain better performance for these devices, instability and degradation factors must be improved. For this purpose various methods have been suggested which include: synthesis of new donor and acceptor materials for use in photoactive blend [7,8], improving the morphology of photoactive layer [9,10], using of interface layers [11,12], and designing new structures for device [13,14].

The other important topics which have been studied in OSCs are: improving reliability [15], increasing reachable solar energy during daytime [16], and to obtain enhanced power conversion efficiency (PCE) [17]. Among these topics, to obtain enhanced PCE is more important. The PCE is defined as the input power (P_{in}) that can convert to output power (P_{out}): $\eta = \frac{P_{out}}{P_{in}} = \frac{FF(V_{oc} \times J_{sc})}{P_{in}}$ and is determined by three parameters: short circuit current density (J_{sc}) as current density in zero voltage conditions, open circuit voltage (V_{oc}) as voltage in zero current conditions and fill factor (FF):$FF = \frac{V_{mpp} \times J_{mpp}}{V_{oc} \times J_{sc}}$. In these equations, V_{mpp} and J_{mpp} are the voltage and current density at maximum output power, respectively [18-20]. The PCE is dependent to charge carriers mobility and many investigation have been done to study the effect of mobility on the OSCs efficiency [21,22].

In so-called bulk hetero-junction (BHJ) OSCs a mixture of donor (usually poly-thiophene derivatives) and acceptor materials (often fullerene derivatives) are used as photoactive (absorber) layer for efficient exciton dissociation [23]. However due to poor absorption in visible region and high cost synthesis of these materials, non-fullerene small molecules materials have been suggested [24,25]. In these devices, active layer is located between two electrodes, hole transport layer (HTL) is located between anode and active layer and electron transport layer (ETL) is located between cathode and active layer to modify the operation and stability [26]. Four fundamental steps are used for describing operation mechanisms of BHJ OSC devices: (1) light absorption and exciton generation, (2) exciton diffusion and exciton splitting, (3) charge transportation and (4) charge collection [27]. From light absorption to collection of charge carriers, some limitations can occur such as absorption losses related to spectral mismatch, thermal

losses, insufficient energy for exciton splitting, and charge recombination, etc. [28]. The most important condition to obtain high efficiency for these devices is sufficient sunlight absorption in absorber layer [29]. Also the most important factor affecting on transportation of charge carriers and their recombination losses is their mobility in photoactive layer [30]. So that in low mobility values, they remain bound to each other through Coulomb potential and recombine before reaching to the electrodes [31].

The simplistic and accurate drift-diffusion model is used for studying the effect of different parameters on the performance of OSCs [32, 33]. With considering constant value for electron to hole mobility ratio, BHJ OSCs characteristics such as V_{oc}, J_{sc}, FF and PCE have been studied by Kirchartz et al. [34].

2. Models and methods

In this manuscript, the effective material approximation has been considered for drift-diffusion simulation of BHJ OSCs with anode located at x=0 and cathode located at x=d. This is an approximation where the blend has been behaved as a homogeneous material, removing real interfaces between the donor and acceptor. The ionization potential (IP) defined as valance energy state is determined by the highest occupied molecular orbital (HOMO) of the donor. The electron affinity (EA) defined as conduction energy state is determined by the lowest unoccupied molecular orbital (LUMO) of the acceptor. The energy gap of effective material (E_g^{DA}) is defined as difference between these levels (Fig. 1) [35-37]. The absorption of solar light is done in the donor material, then electrons are excited from HOMO of the donor to LUMO of the acceptor and electron-hole pairs (known as excitons) are formed. The balance between HOMO of the donor and LUMO of the acceptor is in the range of 0.1 – 1.4 eV. With considering enough dropping for potential energy in the acceptor-donor interface, generated excitons diffuse to this interface to split into free charge carriers [38]. After splitting, these charge carriers are transported to the electrodes while they may be encountered with recombination and trapping effects in their pathway.

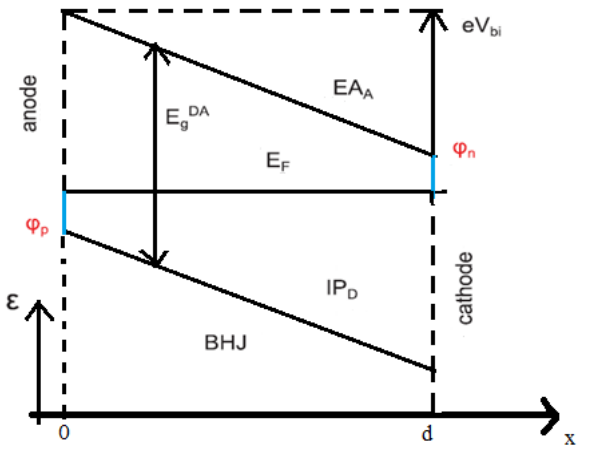

Fig. 1. A bulk hetero-junction (BHJ) OSC as effective medium between two metal contacts (colour online)

The drift–diffusion (equations 1 and 2), Poisson (equation 3) and continuity (equations 4 and 5) equations are written as follows:

$$J_n = -qn\mu_n \frac{\partial}{\partial x}\Psi + qD_n \frac{\partial}{\partial x} n \tag{1}$$

$$J_p = -qp\mu_p \frac{\partial}{\partial x}\Psi - qD_p \frac{\partial}{\partial x} p \tag{2}$$

$$\frac{\partial^2}{\partial x^2}\Psi(x) = \frac{q}{\varepsilon}[n(x) - p(x) + N_D^+ - N_A^-] \tag{3}$$

$$\frac{\partial}{\partial x} J_n(x) = -q[G - R_n] \tag{4}$$

$$\frac{\partial}{\partial x} J_p(x) = q[G - R_p] \tag{5}$$

In these equations, q is elementary charge, μ_n and μ_p are electron and hole mobility and D_n and D_p are electron and hole diffusion coefficients respectively.

In Poisson equation, electrostatic potential $\Psi(x)$ is related to electron (n(x)), hole (p(x)), ionized acceptor (N_A^-) and donor (N_D^+) densities and ε is dielectric constant. The boundary conditions for poisson equation are written as follows [39,40]:

$$\Psi(d) - \Psi(0) = \frac{1}{q} E_g^{DA}\text{-V} \tag{6}$$

$$p(0) = N_V \exp\left(-\frac{\varphi_p}{k_B T}\right) \tag{7}$$

$$n(0) = N_C \exp\left(\frac{-E_g^{DA} - \varphi_p}{k_B T}\right) \tag{8}$$

$$n(d) = N_C \exp\left(-\frac{\varphi_n}{k_B T}\right) \tag{9}$$

$$p(d) = N_V \exp\left(\frac{-E_g^{DA} - \varphi_n}{k_B T}\right) \tag{10}$$

where V and d are applied potential and active layer thickness respectively, N_c and N_v are effective density of states (DOS) in LUMO and HOMO levels respectively, T is as absolute temperature and k_B is as Boltzmann's constant. However in BHJ OSCs, potential barriers at the donor material/anode and acceptor material/cathode interfaces must be reduced to most charge carrier extraction. Therefore the contacts of these devices are usually ohmic and injection barriers for electrons (φ_n) and holes (φ_p) have been neglected.

In continuity equations, $J_n(x)$ and $J_p(x)$ are electron and hole current densities respectively, G is optical generation rate of free charge carriers and R_n (R_P) is bimolecular recombination rate of free electrons (holes) also called direct electron-hole recombination:

$$R_{n,p} = \gamma(np - n_i^2) \tag{11}$$

$$G = k_{diss} n_{exc} \quad (12)$$

In this equations $k_{diss}n_{exc}$ describes the exciton dissociation rate into free charge carriers, n_{exc} is local exciton density and γ and $n_i = \sqrt{N_c N_v}\ \exp[-\frac{E_g^{DA}}{2k_B T}]$ are recombination constant and intrinsic charge carrier density respectively. According to the Langevin theory γ is given as follows:

$$\gamma = \frac{q(\mu_n + \mu_p)}{\varepsilon} \quad (13)$$

with ε as permittivity of the material [41-43].

In BHJ devices, local rate equation for n_{exc} is written as:

$$G_{R(n,p)} + G_{optical} = k_{dec} n_{exc} + k_{diss} n_{exc} \quad (14)$$

In this equation, $G_{optical}$ and $k_{dec}n_{exc}$ describe constant generation rate of excitons through sunlight absorption, and decay rate of bound electron-hole pairs to the ground state (exciton recombination rate or geminate recombination) through the radiative and non-radiative processes. Also $G_{R(n,p)} = R_{n,(p)}$ is generation rate of excitons equal to the free electron-hole pair recombination rate ($R_{n,(p)}$). In the case of geminate recombination, the consequences of a so-called charge transfer (CT) state are considered. This bound electron/hole pair with binding energy E_B is an intermediate state. The CT dissociation and recombination are proportional to its density n_{exc} and described by the rates k_{diss} and k_{dec}.

In efficient splitting mechanism due to dissociation of each exciton into electron-hole pair it is possible to relate the free charge carrier drift-diffusion equations to the exciton generation rate directly. But in practice, the efficient splitting mechanism is not possible and part of the excitons quench before reaching to the donor-acceptor interface. In steady state condition, the electron-hole pair generation is a result of the balance between processes of exciton splitting and geminate recombination. The electron-hole pair generation rate can be given with Onsager-Braun model [44,45]. In this model the influence of the electric field (F), distance between the bound charges of the exciton (x) and temperature is considered on the probability of the exciton dissociation (p(x,F,T)):

$$p(x,F,T) = \frac{k_{diss}(x,F,T)}{k_{diss}(x,F,T) + k_{dec}} \quad (15)$$

$$k_{diss}(x,F,T) = \frac{3\gamma}{4\pi x^3} \exp\left(-\frac{U_b}{k_B T}\right) \frac{J_1(2\sqrt{-2b})}{\sqrt{-2b}} \quad (16)$$

with $U_b = \frac{q^2}{(4\pi\varepsilon x)}$ as exciton binding energy, J_1 as the first order Bessel function and $b = \frac{q^3 F}{(8\pi\varepsilon_r k_B^2 T^2)}$ as field parameter.

In disorder materials, the charge-separation distance is not constant. Therefore, the overall exciton dissociation probability is optained with using a spherically averaged Gaussian distribution as follows:

$$P(F,T) = \frac{4}{\sqrt{\pi}a^3} \int_0^\infty p(x,F,T) x^2 e^{-(\frac{x}{a})^2} dx \quad (17)$$

In this equation, parameter "a" denotes the charge-separation distance in maximum value conditions for probability of Gaussian function.

3. Results and discussion

In this study the conventional P3HT:PCBM based BHJ OSC with the structure of:

ITO (100 nm) / PEDOT:PSS (50 nm) / P_3HT: PCBM (210 nm) / TiO_x (50 nm) / Al (100 nm) has been simulated. The simulation has been done in constant temperatue (300K) for insident light intensity of 0.59 Wcm^{-2}. The optical and electrical parameters of the materials have been introduced in Table 1. In this simulation, the mobility of charge carriers has been changed from 1×10^{-6} to 1 $\frac{cm^2}{V.s}$ for studying their effect on the function of OSCs [46-53].

Table 1. The quantities used in device simulation

Quantity	Symbol	Value
Dielectric constant	ε_r	3.8
Relaxation rate	k_r	1.5×10^6 1/s
Exciton charge-separation distance	a	1.3 nm
LUMO of PCBM	E_C	3.7 eV
Electron effective density of states	N_C	$1.28\times 10^{27} 1/m^3$
HOMO of P_3HT	E_V	5.8 eV
Hole effective density of states	N_V	$2.86\times 10^{25} 1/m^3$
Al workfunction	φ	3.7 eV
ITO workfunction	φ	5 eV
Ag workfunction	φ	4.5 eV
Conduction band of PEDOT:PSS	LUMO	2.9 eV
Valance band of PEDOT:PSS	HOMO	5.1 eV
Conduction band of Tio_x	LUMO	4.7 eV
Valance band of Tio_x	HOMO	7.9 eV

The curve of J_{sc} in terms of one charge carrier (electron or hole) mobility at constant values considered for mobility of other charge carrier has been showed in Fig. 2. As can be seen from this figures, increasing the electron or hole mobility lead to enhanced J_{sc} which is consistent with simulation results in references [46-53]. According to equation 13, bulk recombination rate is dependent to slower charge carrier mobility. Therefore

with increasing this quantity, the increased bulk recombination rate and decreased J_{sc} can be resulted. On the other hand with increasing charge carriers mobility, their extraction would be easier and consequently reduced concentration inside the active layer can be resulted. This leads to reduced bulk recombination rate and increased J_{sc}. In fact the mobility has a two-fold effect on J_{sc}. However, it has been expressed with simulation results that at low mobility values, the priority is with extraction of charge carriers and with increasing of charge carrier mobility J_{sc} has been increased.

Another issues observed in Fig. 2 are as follows: At high values for electron or hole mobility with assuming constant values for other charge carrier mobility, J_{sc} has been saturated and reached to its maximum value. The reason is that in high mobility values, Langevin recombination of charge carriers becomes more important and competition between the extraction of charge carriers and their recombination has been reached to equilibrium state. At lower values considered for electron or hole mobility, increasing the mobility of other charge carrier has negligible effect on J_{sc}. With considering an average value for mobility of one carrier and increasing the mobility of other carrier, the gradual increase of J_{sc} has been observed. The reason is that at low mobility values, the required time for charge carriers reaching to the contacts is more than their lifetime, which lead to limited J_{sc} [34, 54, 55].

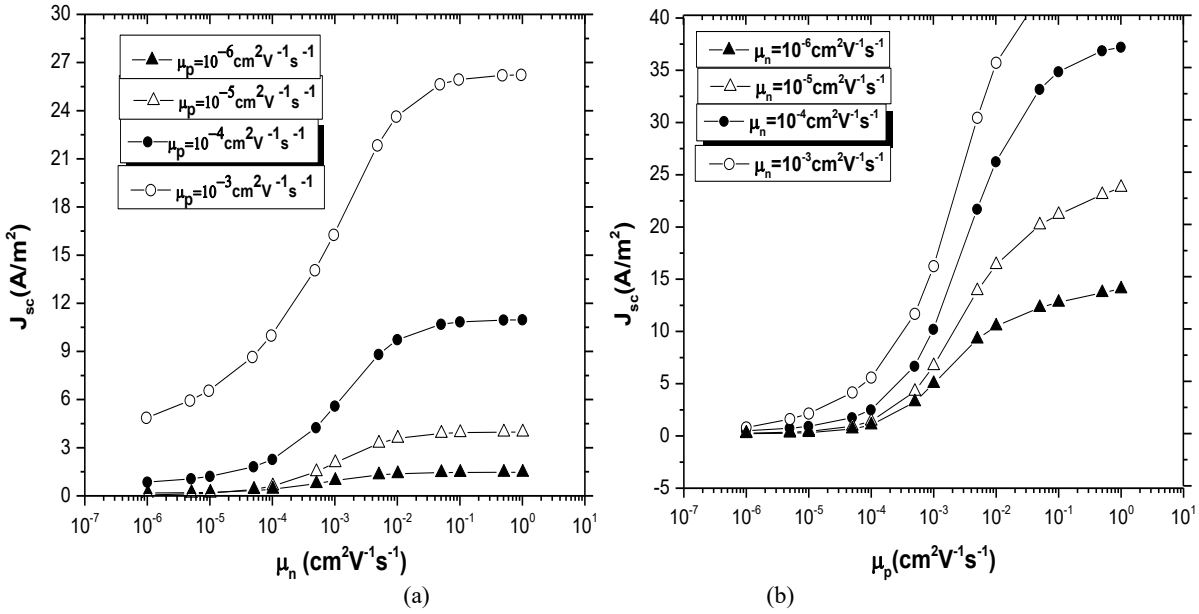

Fig. 2. The comparison of charge carriers mobility effect on J_{sc} of OSCs

In disorder systems, the binding energy of electron-hole pairs is variable. In these devices for charge transfer states with efficient coupling and different binding energies, the charge carriers have been flowed from regions with higher band gap to the lower band gap. This leads to lower open circuit voltage for BHJ OSCs. In the simulation of these devices, the disorder is considered with integrating of electron-hole pair dissociation probability over the separation distances. In these devices, the charge transfer states can' not interact straightly and the coupling occurs alone between free charges. Therefore the bulk recombination is effective on the process [34].

The curve of V_{oc} in terms of one charge carrier (electron or hole) mobility at constant values considered for mobility of other charge carrier has been illustrated in Fig. 3. As can be seen from this figure, by considering constant values for hole mobility and increasing the mobility of electron, the V_{oc} has been decreased steadily, while by considering constant values for electron mobility and increasing the mobility of hole, the V_{oc} has been increased steadily. These results are consistent with references [46-53]. The continuous reduction of V_{oc} with increasing electron mobility is related to the existence of other loss mechanism moreover than bulk recombination. With increasing the electron mobility, up to limit equal values for electron and hole mobility, bulk recombination rate has been increased and consequently V_{oc} has been decreased. The reason is that with increasing the electron mobility, the charge carriers mobility get closer to each other and their interaction rises. With increasing the electron mobility beyond a certain value, bulk recombination rate has been reduced due to the imbalanced values for charge carriers mobility. It seems that, reduced bulk recombination rate will lead to the increased V_{oc} but due to recombination of electrons with holes in anode V_{oc} has been decreased.

By considering constant values for electrons mobility and increasing the mobility of holes, V_{oc} has been increased. This is related to imbalanced values of charge carriers mobility and their lower interaction which lead to decreased bulk recombination rate. Also, recombination of holes in cathode can lead to reduced charge carriers density and reduced bulk recombination rate inside the active layer. However, in this case the recombination of holes in cathode is negligible because of the thick active layer.

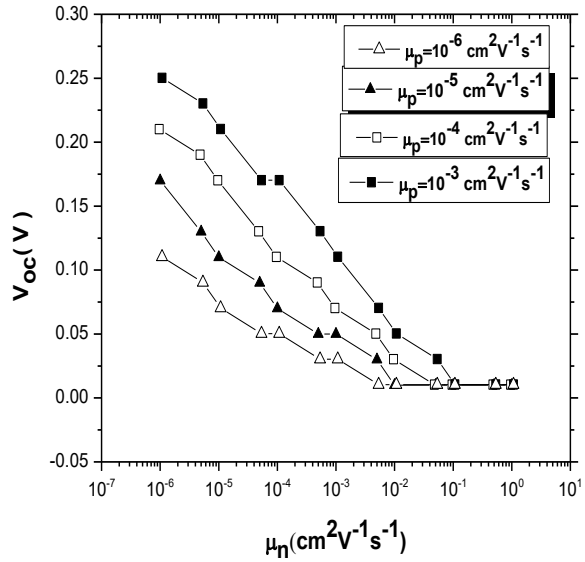

(a)

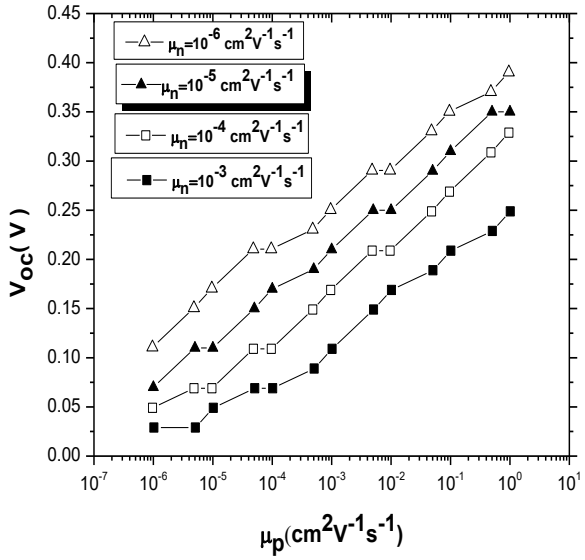

(b)

Fig. 3. The comparison of charge carriers mobility effects on V_{oc} of OSCs

The PCE diagrams in terms of one charge carrier (electron or hole) mobility in constant values considered for mobility of other charge carriers have been shown in Fig. 4. As can be seen from this figure, increasing the mobility of charge carriers leads to a slow increase in the efficiency towards the maximum point. After the maximum point, PCE has been decreased with increasing the mobility. Also when the constant value considered for mobility of one charge carrier is very small (10^{-6} cm^2V^{-1} s^{-1}), increasing the mobility of other carrier has a little effect on PCE curve. With increasing the constant value this influence would be stronger. The simulation results for PCE are consistent with simulation results in references [46-53].

In order to obtain OSCs with higher PCE a maximum number of generated charge carriers should be collected by contacts. For this purpose it is necessary to improve the mobility of charge carriers. In lower values considered for mobility of charge carriers, the time needed for reaching of them to the respective contacts is higher than their lifetime. This factor limits PCE of the device. With increasing the mobility of charge carriers this restriction is removed and PCE of the device has been increased until reaching to the optimal point. After the optimal point with increasing the mobility of charge carriers, PCE of the device has been decreased due to the efficient recombination of charge carriers in opposite contacts.

The maximum PCE of device is obtained in equal values for charge carriers mobility ($\mu_n = \mu_p = 10^{-3} cm^2 V^{-1} s^{-1}$). Thus the optimal point corresponds to the balanced electron and hole mobility. This indicates that distribution of photo-generated excitons is symmetric and created electron-hole pairs are in equal distance from contacts. The optimal point of the efficiency curve is defined as the tradeoff between increasing of short circuit current density (J_{SC}) and decreasing of open circuit voltage (V_{OC}).

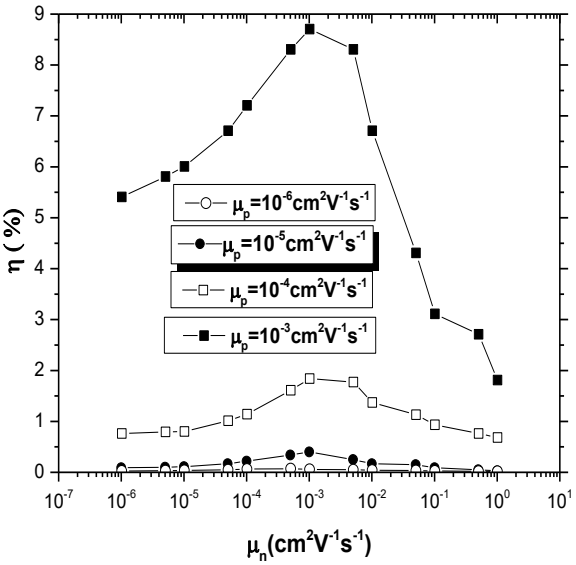

(a)

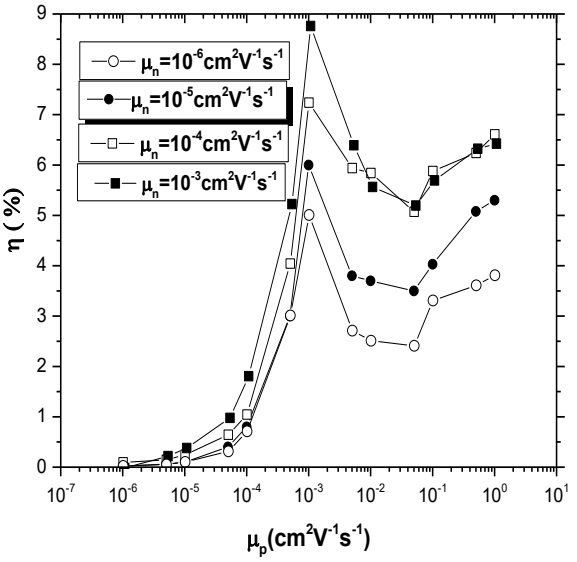

(b)

Fig. 4. The comparison of charge carriers mobility effects on PCE of OSCs

The FF diagrams in terms of one charge carrier (electron or hole) mobility in constant values considered for mobility of other charge carrier have been shown in Fig. 5. These figure shows that FF has been increased with increasing the mobility of charge carriers due to decreasing of direct recombination rate. This result is consistent with simulation results in references [46-53].

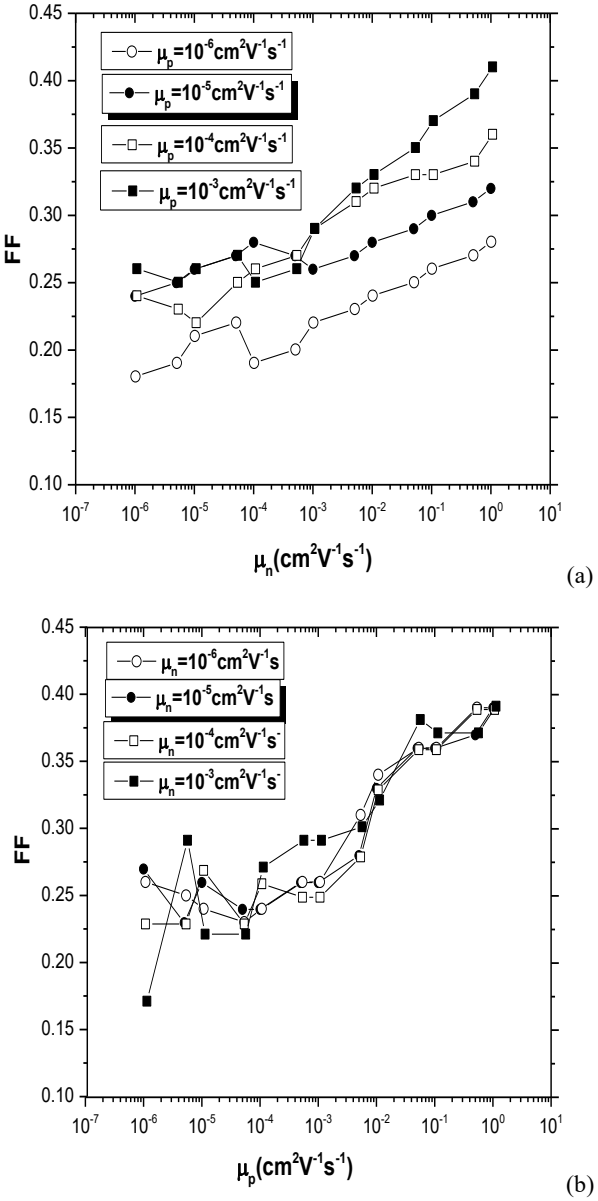

Fig. 5. The comparison of charge carriers mobility effects on FF of OSCs

4. Conclusion

Increasing the mobility of charge carriers lead to enhanced J_{sc}. The optimum point of J_{sc} curve has been obtained at the highest mobility values of one charge carrier when constant values have been considered for mobility of other charge carrier. With considering constant mobility values for holes and increasing the mobility of electrons, V_{oc} has been decreased. While with considering constant mobility values for electrons and increasing the mobility of holes, V_{oc} has been increased. With considering an average value for mobility of one charge carrier and increasing the mobility of other charge carrier PCE curve has been increased until its optimum point. After the optimum point, the PCE curve has been decreased with increasing mobility. At low constant values considered for mobility of one charge carrier (10^{-6} $cm^2V^{-1}s^{-1}$), increasing the mobility of other charge carrier has negligible effect on PCE curve. With increasing the constant value for mobility of one charge carrier this effect would be important. Increasing the mobility of charge carriers lead to increased FF due to decreasing of direct recombination rate.

References

[1] Y. Tong, Z. Xiao, X. Du, C. Zuo, Y. Li, M. Lv, Y. Yuan, C. Yi, F. Hao, Y. Hua, T. Lei, Q. Lin, K. Sun, D. Zhao, C. Duan, X. Shao, W. Li, H. Yip, Z. Xiao, B. Zhang, Q. Bian, Y. Cheng, S. Liu, M. Cheng, Z. Jin, S. Yang, L. Ding, Sci. China Chem. **63**, 1 (2020).

[2] S. Rafique, S. M. Abdullah, K. Sulaiman, M. Iwamoto, Renewable and Sustainable Energy Reviews **84**, 43 (2018).

[3] M. Riede, D. Spoltore, K. Leo, Adv. Energy Mater. **11**, 2002653 (2021).

[4] K. S. Santhoshi Kiran, V. Preethi, S. Kumar, Materials Today Proceedings **56**, 3826 (2022).

[5] L. Duan, A. Uddin, Adv. Sci.**7**, 1903259 (2020).

[6] M. Wu, B. Ma, S. Li, J. Han, W. Zhao, Adv. Funct. Mater. **33**, 2305445 (2023).

[7] Y. Li, W. Huang, D. Zhao, L. Wang, Z. Jiao, Q. Huang, P. Wang, M. Sun, G. Yuan, Molecules **27**, 1800 (2022).

[8] G. P. Kini, S. J. Jeon, D. K. Moon, Adv. Funct. Mater. **31**, 2007931 (2021).

[9] M. Yang, S. Fu, L. Wang, M. Ren, H. Li, S. Han, X. Lu, F. Lu, J. Tong, J. Li, Opt. Mater. **137**, 113503 (2023).

[10] K. Weng, L. Ye, L. Zhu, J. Xu, J. Zhou, X. Feng, G. Lu, S. Tan, F. Liu, Y. Sun, Nat. Commun. **11**, 2855 (2020).

[11] Z. Yin, J. Wei, Q. Zheng, Adv. Sci. **3**, 1500362 (2016).

[12] H. Tang, Y. Bai, H. Zhao, X. Qin, Z. Hu, C. Zhou, F. Huang, Y. Cao, Adv. Mat. **36**, 2212236 (2024).

[13] Jin Su Park, Geon-U. Kim, Seungjin Lee, Jin-Woo Lee, Sheng Li, Jung-Yong Lee, Bumjoon J. Kim, Adv. Mater. **34**, 2201623 (2022).

[14] Z. He, B. Xiao, F. Liu, H. Wu, Y. Yang, S. Xiao, C. Wang, T. P. Russell, Y. Cao, Nat. Photonics **9**, 174 (2015).

[15] H. Momeni, N. Sadoogi, M. Farrokhifar, H. F. Gharibeh, IEEE Transactions on Industrial

Informatics **16**(8), 5300 (2020).
[16] M. Dadras, M. Farrokhifar, International Journal of Renewable Energy Research **5**(3), 766 (2015).
[17] N. Sadoogi, A. Rostami, M. Dolatyari, G. Rostami, Optical and Quantum Electronics **47**, 3871 (2015).
[18] Y. Firdaus, V. M. Le Corre, J. I. Khan, Z. Kan, F. Laquai, P. M. Beaujuge, T. D. Anthopoulos, Adv. Sci. **6**, 1802028 (2019).
[19] N. K. Elumalai, A. Uddin, Energy Environ. Sci. **9**, 391 (2016).
[20] V. A. Trukhanov, V. V. Bruevich, D. Y. Paraschuk, Sci. Rep. **5**, 11478 (2015).
[21] H. Mehdizadeh-Rad, J. Singh, Journal of Materials Science: Materials in Electronics **30**, 10064 (2019).
[22] D. Glowienka, J. Szmytkowski, Chemical Physics **503**, 31 (2018).
[23] J. Ajayan, D. Nirmal, P. Mohankumar, M. Saravanan, M. Jagadesh, L. Arivazhagan, Superlattices and Microstructures **143**, 106549 (2020).
[24] T. Liu, R. Ma, Z. Luo, Y. Guo, G. Zhang, Y. Xiao, T. Yang, Y. Chen, G. Li, Y. Yi, X. Lu, H. Yan, B. Tang, Energy & Environmental Science **13**, 2115 (2020).
[25] R. Ma, Y. Chen, T. Liu, Y. Xiao, Z. Luo, M. Zhang, S. Luo, X. Lu, G. Zhang, Y. Li, H. Yan, K. Chen, Journal of Materials Chemistry C **8**, 909 (2020).
[26] H. Kang, G. Kim, J. Kim, S. Kwon, H. Kim, K. Lee, Advanced Materials **28**, 7821 (2016).
[27] I. C. Ghosekar, G. C. Patil, Semi. Sci. Technol. **36**, 045005 (2021).
[28] Y. Xu, H. Yao, L. Ma, J. Wang, J. Hou, Rep. Pro. Phys. **83**, 082601 (2020).
[29] J. Jing, S. Dong, K. Zhang, Z. Zhou, Q. Xue, Y. Song, Z. Du, M. Ren, F. Huang, Adv. Energy Mater. **12**, 2200453 (2022).
[30] Mahya Ghorab, Ali Fattah, Mojtaba Joodaki, Optik **267**, 169730 (2022).
[31] Q. Liu, K. Vandewal, Adv. Mater. **35**, 2302452 (2023).
[32] H. Movla, A. Shahalizad, A. R. N. Abad, Optical and Quantum Electronics **47**, 621 (2015).
[33] A. Gagliardi, S. Wang, T. Albes, Organic Electronics **59**, 171 (2018).
[34] T. Kirchartz, B. E. Pieters, K. Taretto, U. Rau, Physical Review B **80**, 035334 (2009).
[35] L. H. Luo, L. G. Wang, Y. L. Liang, L. Zhang, Y. J. Wang, Optoelectron. Adv. Mat. **16**(7-8), 373 (2022).
[36] R. Yahyazadeh, Z. Hashempour, Journal of Optoelectronical Nano Structures **6**(2), 1 (2021).
[37] M. Saleheen, S. M. Arnab, M. Z. Kabir, Energies **9**, 412 (2016).
[38] C. Varun, S. Nidhi, M. Garima, Journal of Nanoelectronics and Optoelectronics **17**, 579 (2022).
[39] C. Liang, Y. Wang, D. Li, X. Ji, F. Zhang, Z. He, Solar Energy Materials & Solar Cells **127**, 67 (2014).
[40] W. Yang, Y. Yao, C. Q. Wu, Organic Electronics **14**, 1992 (2013).
[41] H. Hashemi, M. R. Shayesteh, M. R. Moslemi, Journal of Optoelectronical Nano Structures **6**(1), 71 (2021).
[42] G. C. Wang, L. G. Wang, L. Zhang, Y. Guo, Y. J. Wang, Optoelectron. Adv. Mat. **15**(1-2), 86 (2021).
[43] A. Petersen, T. Kirchartz, T. A. Wagner, Phys. Rev. B **85**, 045208 (2012).
[44] A. Mahmoudloo, Journal of Optoelectronical Nanostructures **7**(4), 1 (2022).
[45] D. Jalalian, A. Ghadimi, A. K. Sarkaleh, Journal of Optoelectronical Nanostructures **5**(2), 65 (2020).
[46] A. Spies, M. List, T. Sarkar, U. Wyrfel, Adv. Energy Mater. **7**, 1601750 (2016).
[47] W. Tress, K. Leo, M. Riede, Phys. Rev. B **85**, 155201 (2012).
[48] A. H. Fallahpour, A. Gagliardi, F. Santoni, D. Gentilini, A. Zampetti, M. Auf der Maur, A. Di Carlo, J. Appl. Phys. **116**, 184502 (2014).
[49] J. T. Shieh, C. H. Liu, H. F. Meng, S. R. Tseng, Y. C. Chao, S. F. Horng, J. Appl. Phys. **107**, 084503 (2010).
[50] S. Zhou, J.-X. Sun, International Journal of Modern Physics B **27**(28), 1350167 (2013).
[51] T. Kirchartz, B. E. Pieters, K. Taretto, U. Rau, Phys. Rev. B **80**, 035334 (2009).
[52] D. Gentilini, A. Gagliardi, M. A. Maur, L. Vesce, D. D'Ercole, T. M. Brown, A. Reale, A. D. Carlo, J. Phys. Chem. C **116**, 1151 (2012).
[53] C. Liang, Y. Wang, D. Li, X. Ji, F. Zhang, Z. He, Solar Energy Materials and Solar Cells **127**, 67 (2014).
[54] M. I. Ibrahim, Z. Ahmad, K. Sulaiman, S. Muniandy, AIP Advances **4**, 057133 (2014).
[55] W. Tress, K. Leo, M. Riede, Physical Review B **85**, 155201 (2012).

*Corresponding author: auobi_ali@yahoo.com